チベット高原での高エネルギー宇宙線の研究

瀧田正人　東京大学宇宙線研究所

平成21年度共同利用成果発表会

@宇宙線研究所　2009.12.19

（For the Tibet ASγCollaboration）

平成21年度チベット実験関係
共同利用研究採択課題一覧

1. チベット高原での高エネルギー宇宙線の研究
   （瀧田正人　東京大学宇宙線研究所）

2. Knee領域一次宇宙線組成の研究
   （柴田槇雄　横浜国立大学大学院工学研究院）

3. 銀河拡散ガンマ線の観測
   （日比野欣也　神奈川大学工学部）

4. チベット実験用シミュレーション計算
   （堀田　直巳　宇都宮大学教育学部）

5. 宇宙線による太陽の影を用いた太陽周辺磁場の時間変動の研究
   （西澤正己　国立情報学研究所人間・社会情報研究系）

6. チベット空気シャワーアレイによる10TeV宇宙線強度の恒星時日周変動の観測
   （宗像一起　信州大学理学部）

チベットグループ共同利用研究経費執行状況

校費:　申請額 480万円　→　配分額 220万円

2002年に完成したTibet-IIIの維持・運転及び高電圧電源クレート1458HPを購入等に使用。

旅費:　申請額 907万円　→　配分額 385万円

宇宙線研での研究打ち合わせや中国出張海外旅費に使用。

ご支援、どうもありがとうございます！

The Tibet ASγ Collaboration

Papers (in refereed journals):

1. Multi-TeV Gamma-Ray Observation from the Crab Nebula Using the Tibet-III Air Shower Array Finely Tuned by the Cosmic-Ray Moon's Shadow
   The Astrophysical Journal, **692**, 61-72 (2009)

2. Chemical Composition of Cosmic Rays around the Knee Observed by the Tibet Air-Shower-Core Detector
   J. Phys. Soc. Jpn., **78**, 206-209 (2009)

3. Recent results on gamma-ray observation by the Tibet air shower array and related topics
   J. Phys. Soc. Jpn., **78**, 88-91 (2009)

4. OBSERVATION OF TeV GAMMA RAYS FROM THE FERMI BRIGHT GALACTIC SOURCES WITH THE TIBET AIR SHOWER ARRAY
   The Astrophysical Journal, Letters, Accepted

International Conference

- **ICRC2009 (Lodz, Poland, 2009) , 14 presentations**

研究目的

大気チェレンコフ望遠鏡と相補的な
広視野（約2sr）連続観測高エネルギー宇宙線望遠鏡

3～100 TeVの高エネルギーガンマ線放射天体の探索、10^{14} ～10^{17} eV の宇宙線の観測から、宇宙線の起源、加速機構の研究を行う。

太陽活動期における“太陽の影”（太陽による宇宙線の遮蔽効果）を観測し、太陽近傍および惑星間磁場の大局的構造を知る。

The Tibet ASγ Collaboration

M.Amenomori(1), X.J.Bi(2), D.Chen(3), S.W.Cui(4), Danzengluobu(5), L.K.Ding(2), X.H.Ding(5), C.Fan(6), C.F.Feng(6), Zhaoyang Feng(2), Z.Y.Feng(7), X.Y.Gao(8), Q.X.Geng(8), Q.B.Gou(2), H.W.Guo(5), H.H.He(2), M.He(6), K.Hibino(9), N.Hotta(10), Haibing Hu(5), H.B.Hu(2), J.Huang(2), Q.Huang(7), H.Y.Jia(7), L.Jiang(8, 2), F.Kajino(11), K.Kasahara(12), Y.Katayose(13), C.Kato(14), K.Kawata(3), Labaciren(5), G.M.Le(15), A.F.Li(6), H.C.Li(4, 2), J.Y.Li(6), C.Liu(2), Y.-Q.Lou(16), H.Lu(2), X.R.Meng(5), K.Mizutani(12, 17), J.Mu(8), K.Munakata(14), A.Nagai(18), H.Nanjo(1), M.Nishizawa(19), M.Ohnishi(3), I.Ohta(20), S.Ozawa(12), T.Saito(21), T .Y.Saito(22), M.Sakata(11), T.K.Sako(3), M.Shibata(13), A.Shiomi(23), T.Shirai(9), H.Sugimoto(24), M.Takita(3), Y.H.Tan(2), N.Tateyama(9), S.Torii(12), H.Tsuchiya(25), S.Udo(9), B.Wang(2), H.Wang(2), Y.Wang(2), Y.G.Wang(6), H.R.Wu(2),L.Xue(6), Y.Yamamoto(11), C.T.Yan(26), X.C.Yang(8), S.Yasue(27), Z.H.Ye(28), G.C.Yu(7), A.F.Yuan(5), T.Yuda(9), H.M.Zhang(2), J.L.Zhang(2), N.J.Zhang(6), X.Y.Zhang(6), Y.Zhang(2), Yi Zhang(2), Ying Zhang(7, 2), Zhaxisangzhu(5) and X.X.Zhou(7)

(1)Department of Physics, Hirosaki University, Japan.
(2)Key Laboratory of Particle Astrophysics, Institute of High Energy Physics, Chinese Academy of Sciences, China.
(3)Institute for Cosmic Ray Research, University of Tokyo, Japan.
(4)Department of Physics, Hebei Normal University, China.
(5)Department of Mathematics and Physics, Tibet University, China.
(6)Department of Physics, Shandong University, China.
(7)Institute of Modern Physics, SouthWest Jiaotong University, China.
(8)Department of Physics, Yunnan University, China.
(9)Faculty of Engineering, Kanagawa University, Japan.
(10)Faculty of Education, Utsunomiya University, Japan.
(11)Department of Physics, Konan University, Japan.
(12)Research Institute for Science and Engineering, Waseda University, Japan.
(13)Faculty of Engineering, Yokohama National University, Japan.
(14)Department of Physics, Shinshu University, Japan.
(15)National Center for Space Weather, China Meteorological Administration, China.
(16)Physics Department and Tsinghua Center for Astrophysics, Tsinghua University, China.
(17)Saitama University, Japan.
(18)Advanced Media Network Center, Utsunomiya University, Japan.
(19)National Institute of Informatics, Japan.
(20)Sakushin Gakuin University, Japan.
(21)Tokyo Metropolitan College of Industrial Technology, Japan.
(22)Max-Planck-Institut fur Physik, Deutschland.
(23)College of Industrial Technology, Nihon University, Japan.
(24)Shonan Institute of Technology, Japan.
(25)RIKEN, Japan.
(26)Institute of Disaster Prevention Science and Technology, China.
(27)School of General Education, Shinshu University, Japan.
(28)Center of Space Science and Application Research, Chinese Academy of Sciences, China.

Our site : Tibet

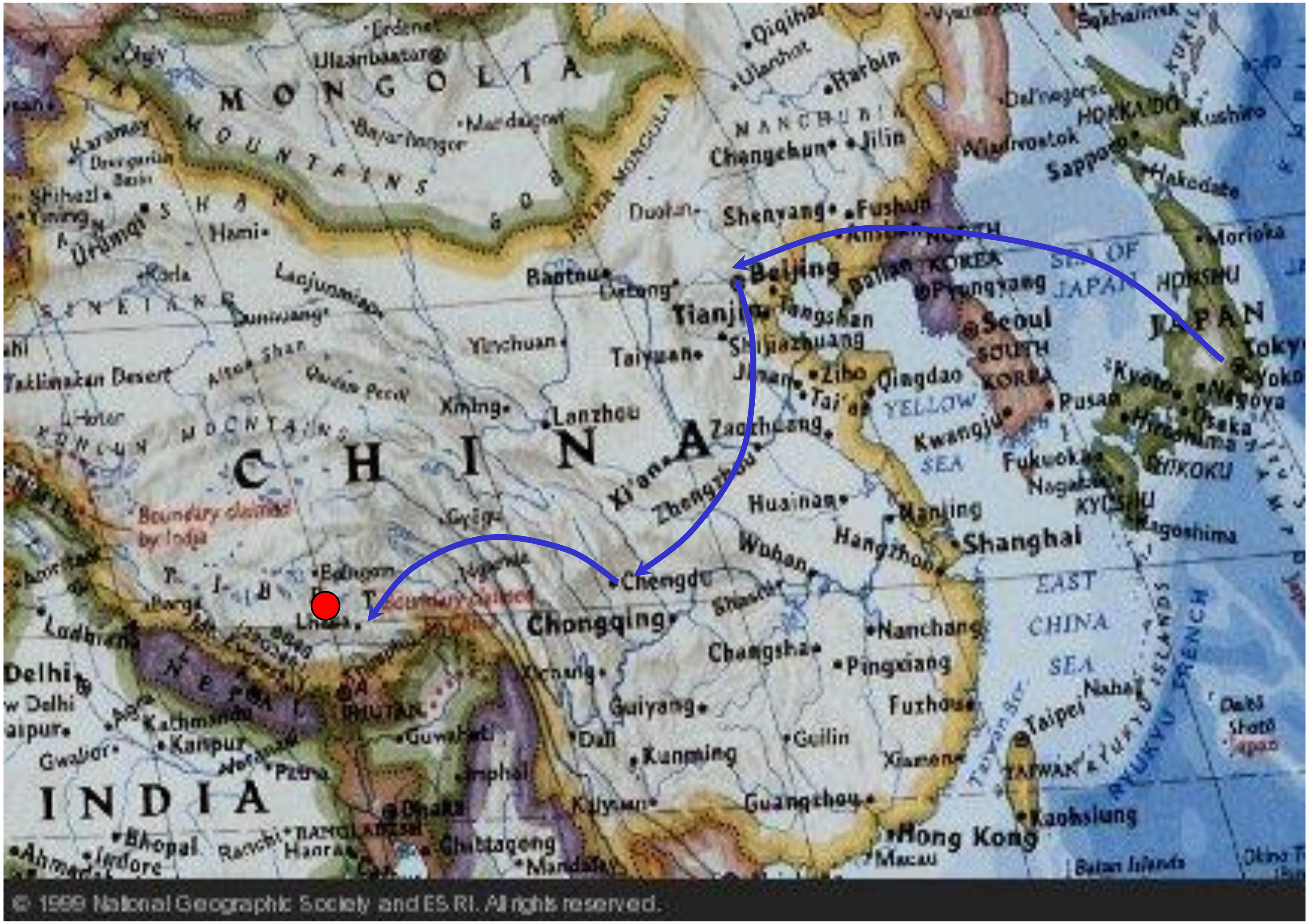

Yangbajing, Tibet, China

90°53**E**, 30°11**N**, 4,300 m a.s.l. (606g/cm^2)

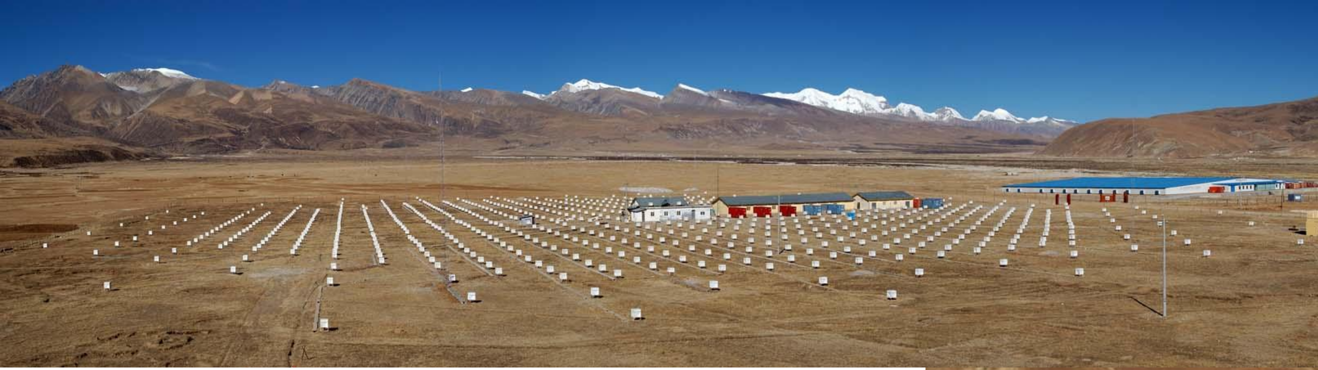

Yangbajing,
Tibet, China

4300 m a.s.l. = 606 g/cm^2

Tibet Air Shower Array

Tibet III (37000 m^2)

Total 789 detectors
Mode Energy
~3 TeV
Angular Resolution
~0.9 deg @ 3 TeV
Trigger Rate
~1700 Hz

月の影による装置性能評価

The Astrophysical Journal,
692, 61–72(2009)

- 絶対エネルギー
- 角度分解能
- ポインティングエラー

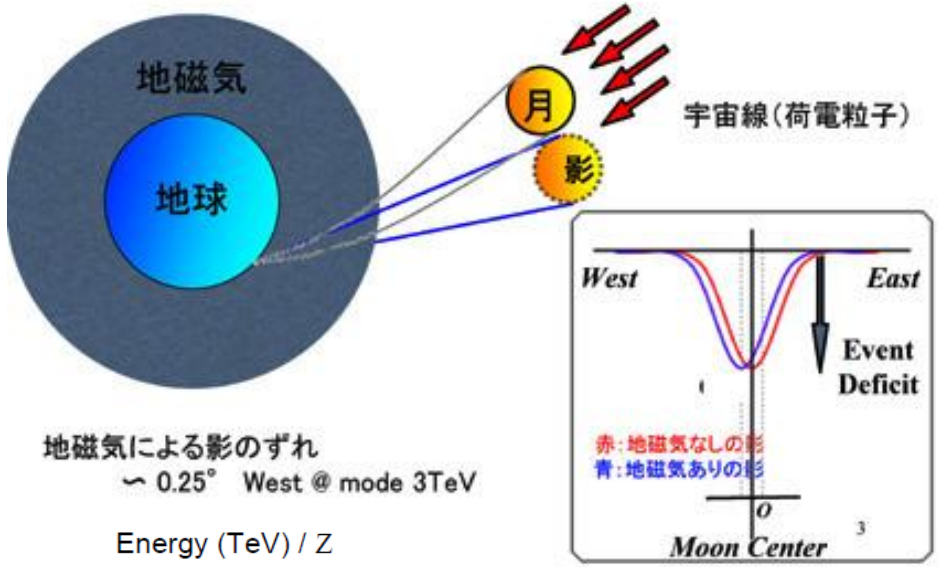

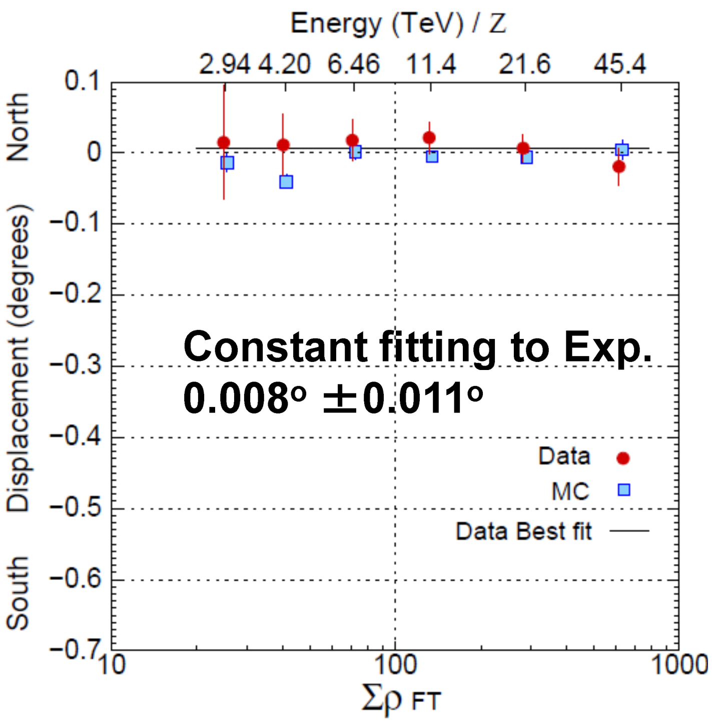

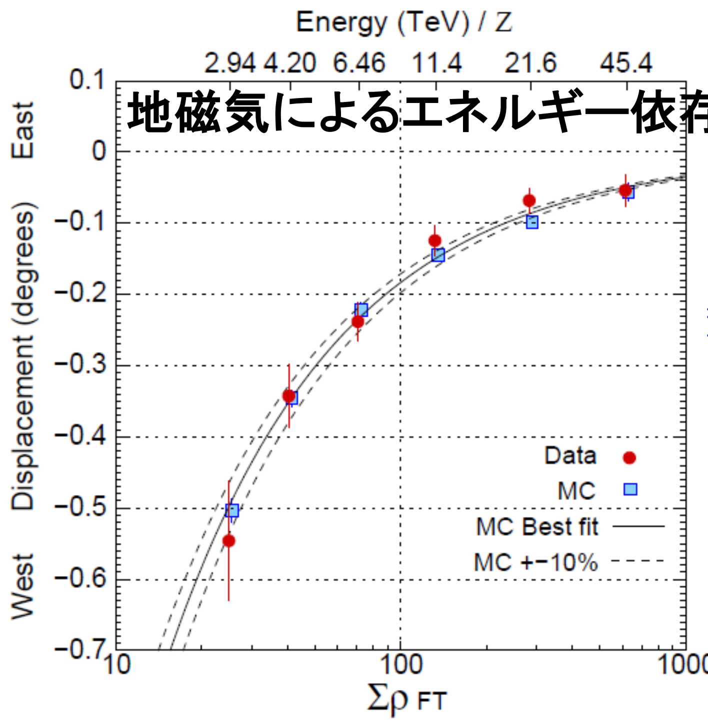

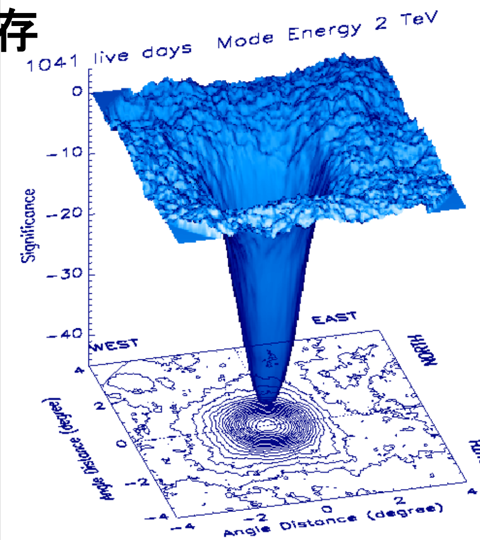

ポインティングエラー
< 0.011°

絶対エネルギーエラー < 12%
+4.5%(±8.6stat.±6.7syst.)%

Knee領域全粒子エネルギースペクトラム

Amenomori *et al.*,
ApJ, **678**, 1165 (2008)

10^{14}eV ～ 10^{17}eV 3桁

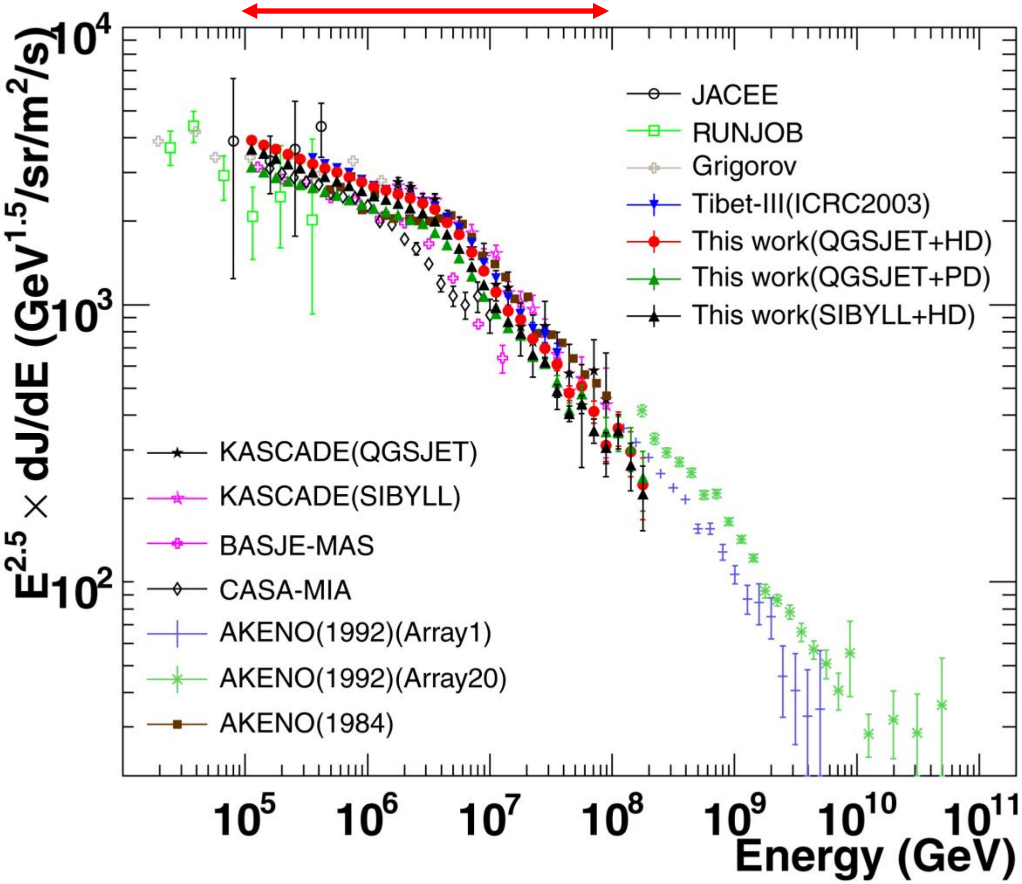

Model	Index of spectrum	Energy range (eV)
QGSJET +HD	−2.67±0.01	< 10^{15} eV
	−3.10±0.01	> 4×10^{15} eV
QGSJET +PD	−2.65±0.01	< 10^{15} eV
	−3.08±0.01	> 4×10^{15} eV
SIBYLL +HD	−2.67±0.01	< 10^{15} eV
	−3.12±0.01	> 4×10^{15} eV

Multiple source model

(Slide from M.Shibata,Y.N.U.)

Cutoff spectrum is written as

$$\frac{dj(E,\varepsilon)}{dE} = j_0 E^{-\gamma} \exp(-\frac{E}{\varepsilon}).$$

Distribution of sources with acceleration limit ε is assumed as,

$$S(x) = \frac{1}{\Gamma(\Delta\gamma)} \frac{1}{x^{1+\Delta\gamma}} \exp(-\frac{1}{x})$$

where $x = \varepsilon/\varepsilon_m$, ε_m is the minimum value of the acceleration limit. $S(x)$ is normalized as

$$\int_0^\infty S(x)dx = 1.$$

Then, superposition of the multiple sources gives following formula for cosmic-ray energy spectrum.

$$\frac{dJ}{dE} = \int_0^\infty \frac{dj(E,\varepsilon)}{dE} S(\frac{\varepsilon}{\varepsilon_m}) \frac{d\varepsilon}{\varepsilon_m} = \frac{j_0 E^{-\gamma}}{(1+E/\varepsilon_m)^{\Delta\gamma}}$$

$\boldsymbol{\varepsilon_m \equiv \varepsilon_b}$

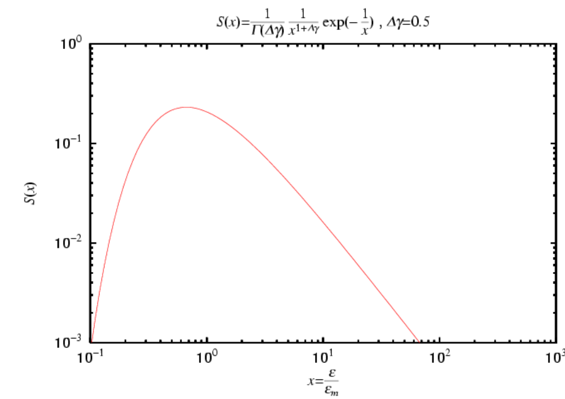

Distribution of acceleration power of cosmic rays

Proton Spectrum

Direct measurement and Tibet combined

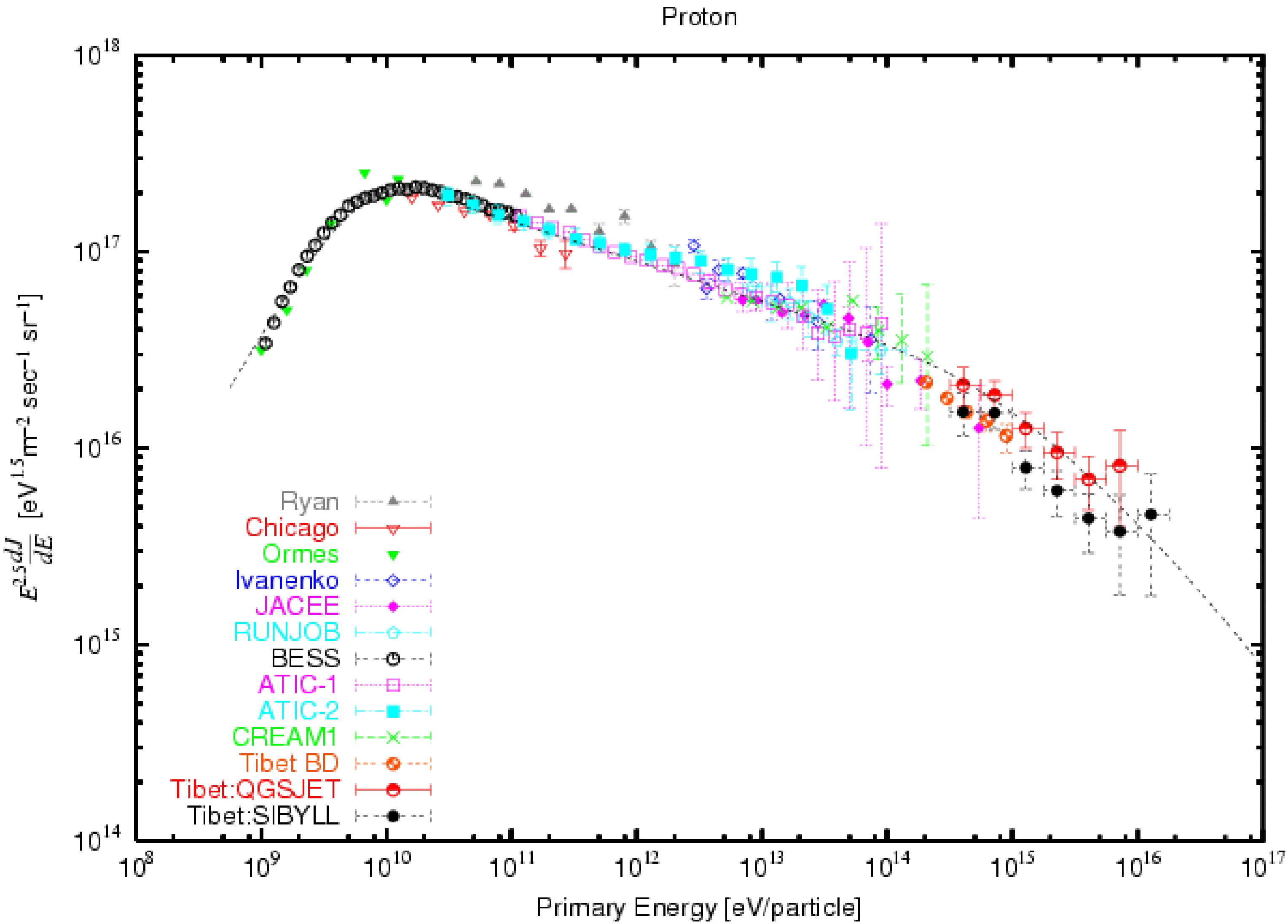

(Slide from M.Shibata,Y.N.U.)

Broken power law formula to describe proton spectrum

$$\frac{dj}{dE} = j_0 E^{-\gamma}[1+\frac{E}{\varepsilon_b}]^{-\Delta\gamma}$$

ε_b : break point (7×10^{14} eV for proton)
$\Delta\gamma$: difference of power index before and after the break point
（ $\Delta\gamma = 0.4$）

(Slide from M.Shibata, Y.N.U.)

All particle spectrum around the knee

(Slide from M.Shibata, Y.N.U.)

CASA/MIA

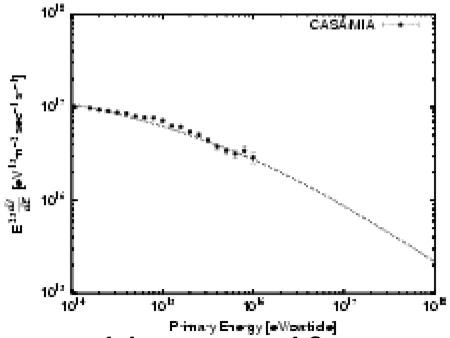

10^{14} 10^{16} 10^{18}

HEGRA

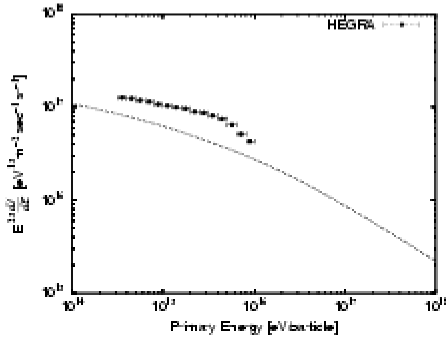

10^{14} 10^{16} 10^{18}

KASCADE

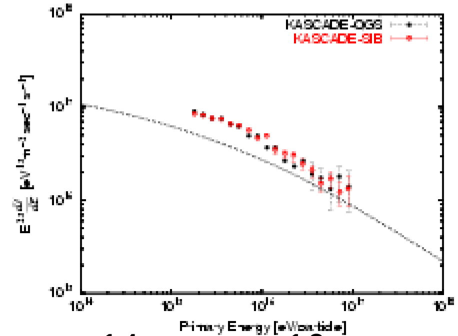

10^{14} 10^{16} 10^{18}

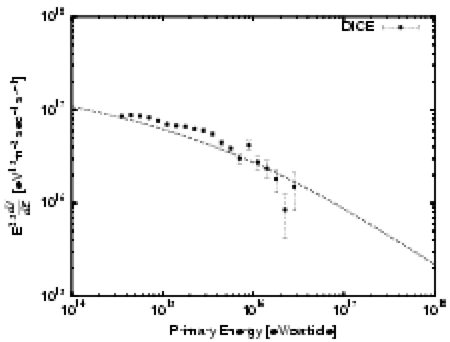

10^{14} 10^{16} 10^{18}

DICE

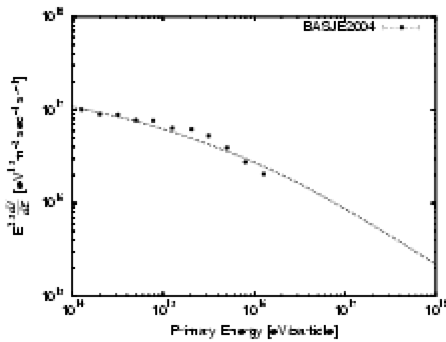

10^{14} 10^{16} 10^{18}

BASJE

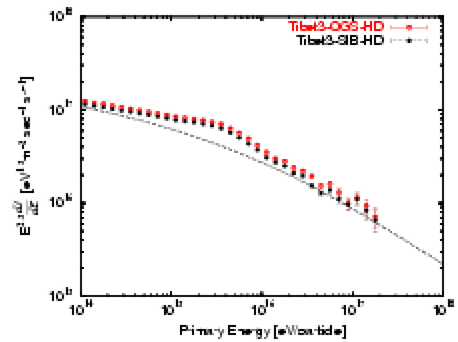

10^{14} 10^{16} 10^{18}

TIBET

Extra component

All data agree if we apply energy scale correction within 20% by normalizing to direct observations.

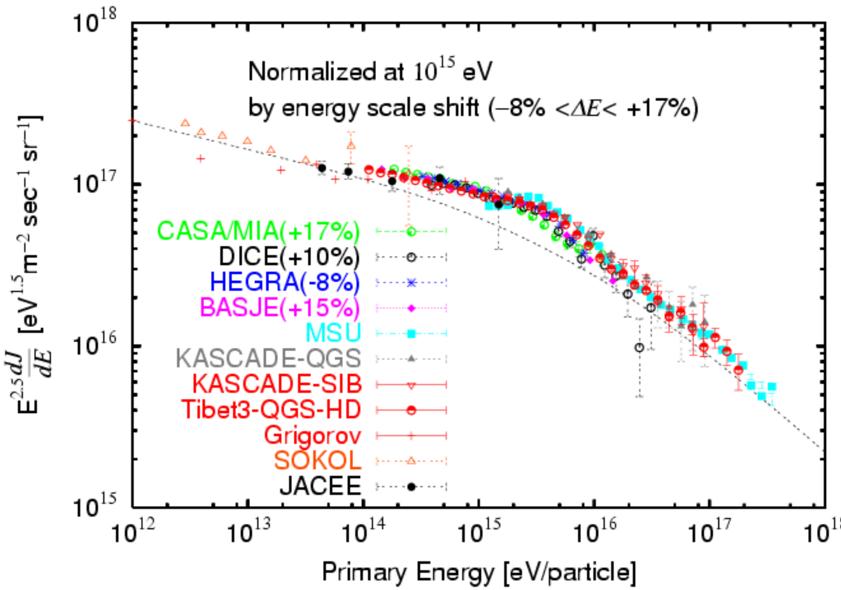

Extra component can be approximated by

$$E^{-2}\exp[-\frac{E}{4\mathrm{PeV}}],$$

suggesting **nearby source(s).**
Since P and He component do not show the excess at the knee, the extra component should be attributed to heavy element such as Fe.

(Slide from M.Shibata, Y.N.U.)

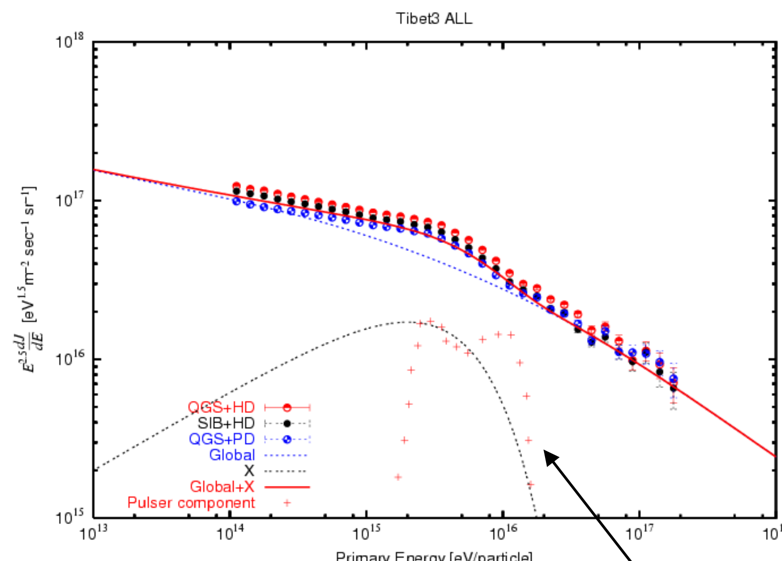

(W.Bednarek and R.J.Protheroe ,2002,APh)

Tibet P +He spectrum does not show excess at the knee

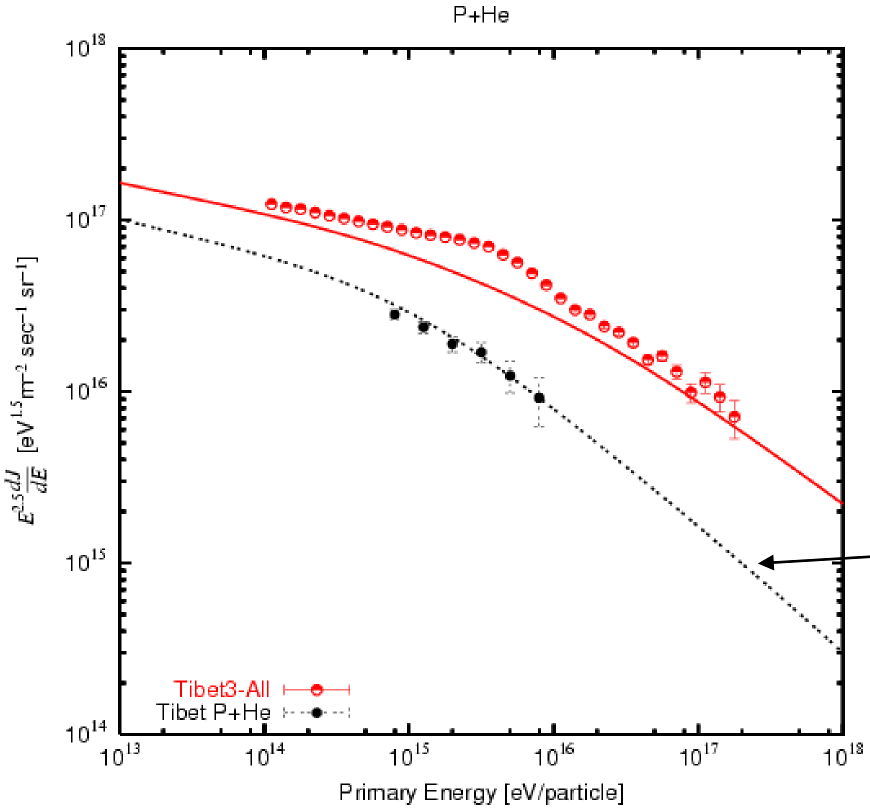

Tibet All particle Data vs. Expected by multiple source model

P+He
Data vs. Expected by multiple source model

(Slide from M.Shibata, Y.N.U.)

(Slide from M.Shibata Y.N.U.)

Chemical composition of SN ejecta

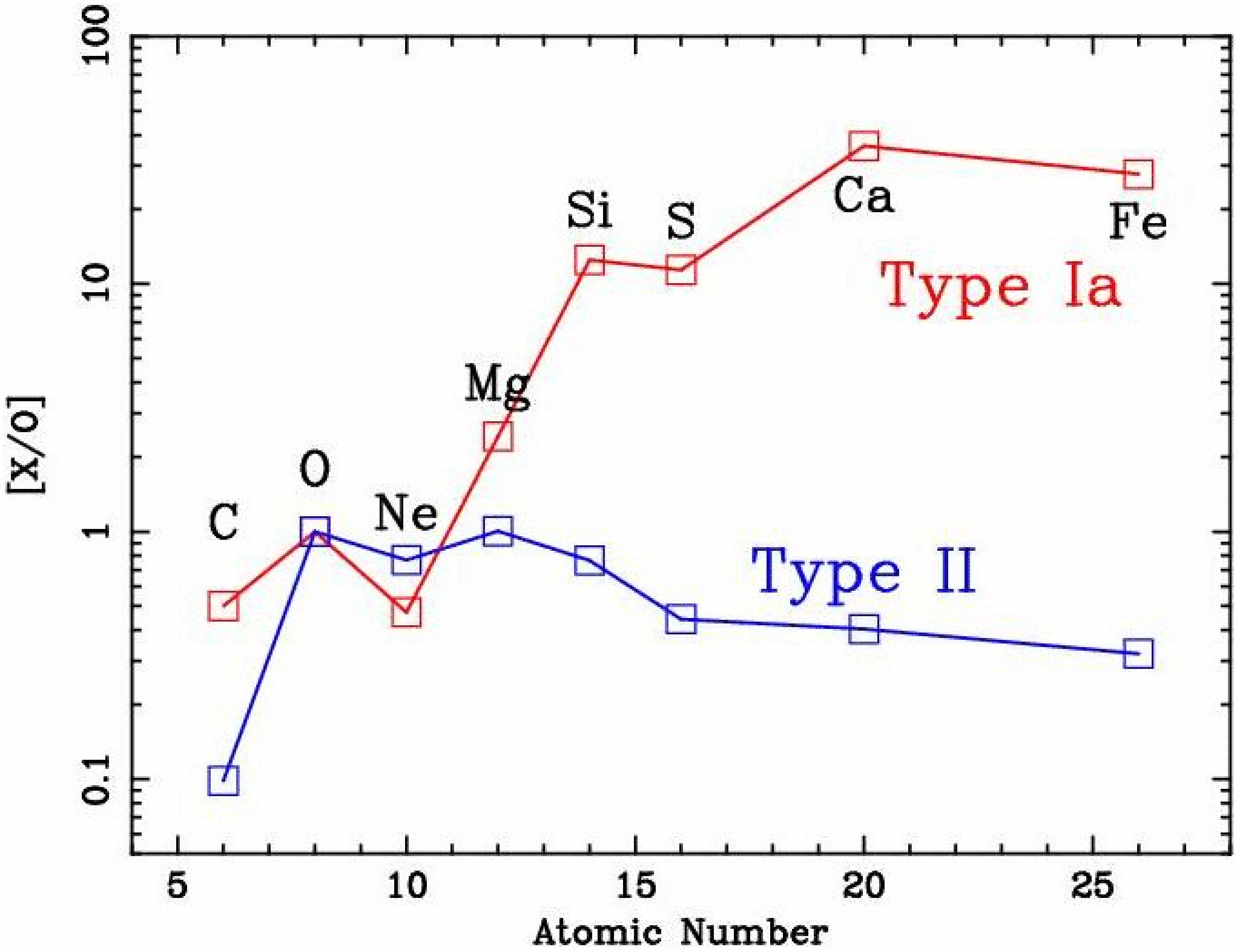

(Nomoto,K et al. Nucl. Phys. A, 621, 467, 1997)

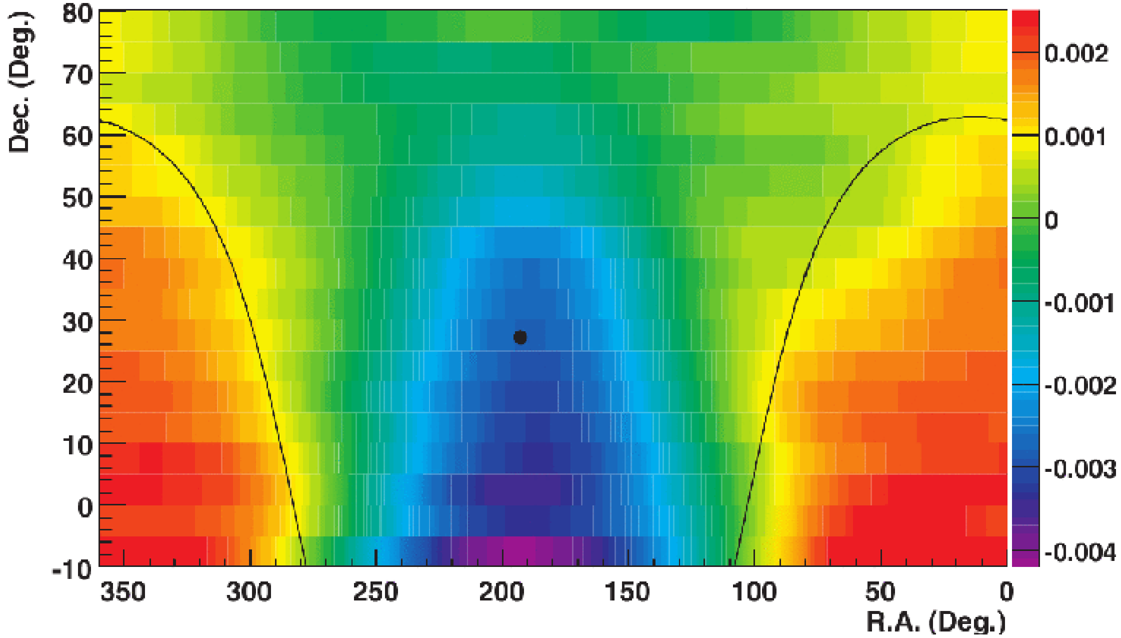

Milagro sidereal anisotropy (6TeV)

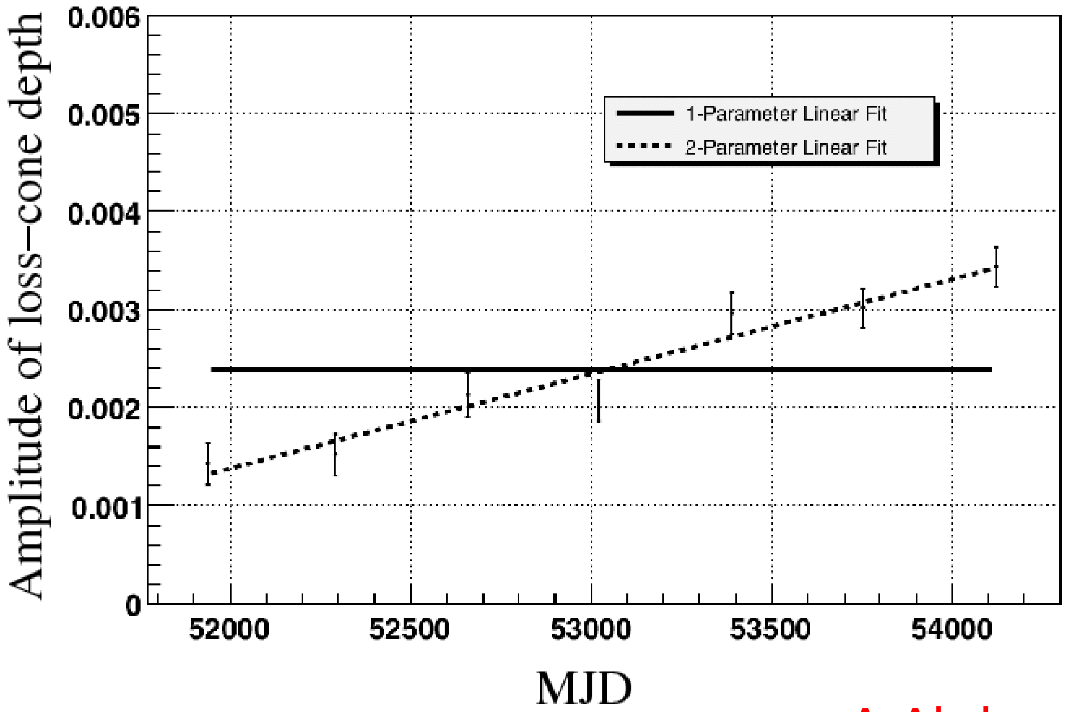

2000-2007 DATA
Yeary variation of Loss Cone depth!

A.Abdo et al., ApJ **698**(2009)2121.

Anisotropy of galactic cosmic rays

I: tain-in, II:loss cone, III: Cygnus

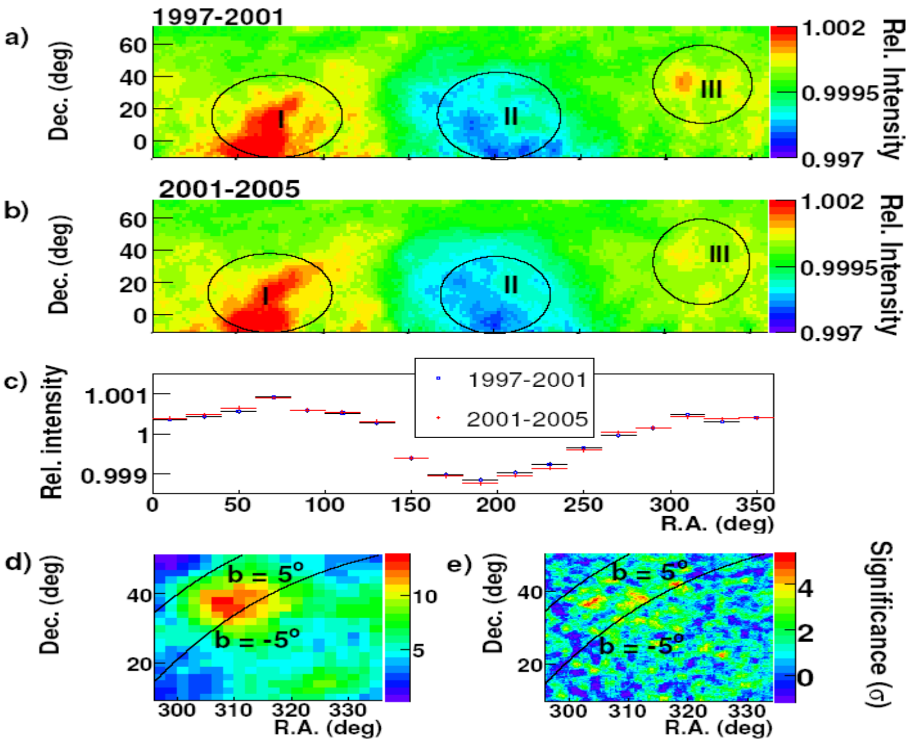

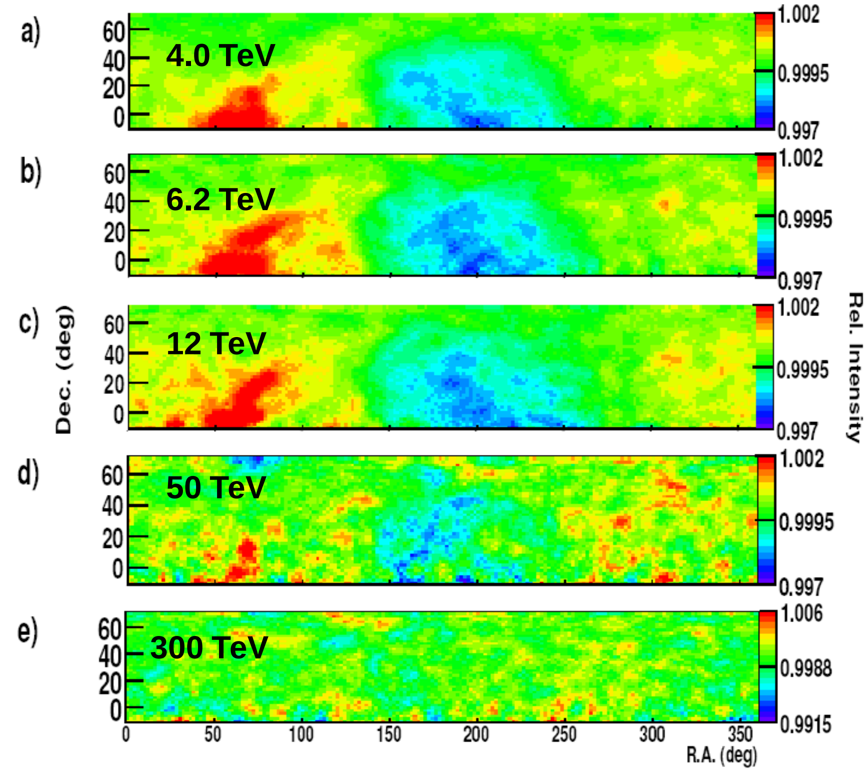

i) No significant temporal variation

iii) Corotation (CR and Galaxy)

ii) New Anisotropy in the Cygnus region

M. Amenomori et al., Science, **V**314, pp.439 – 443 (**2006**)

Yearly variation of Loss Cone amplitude

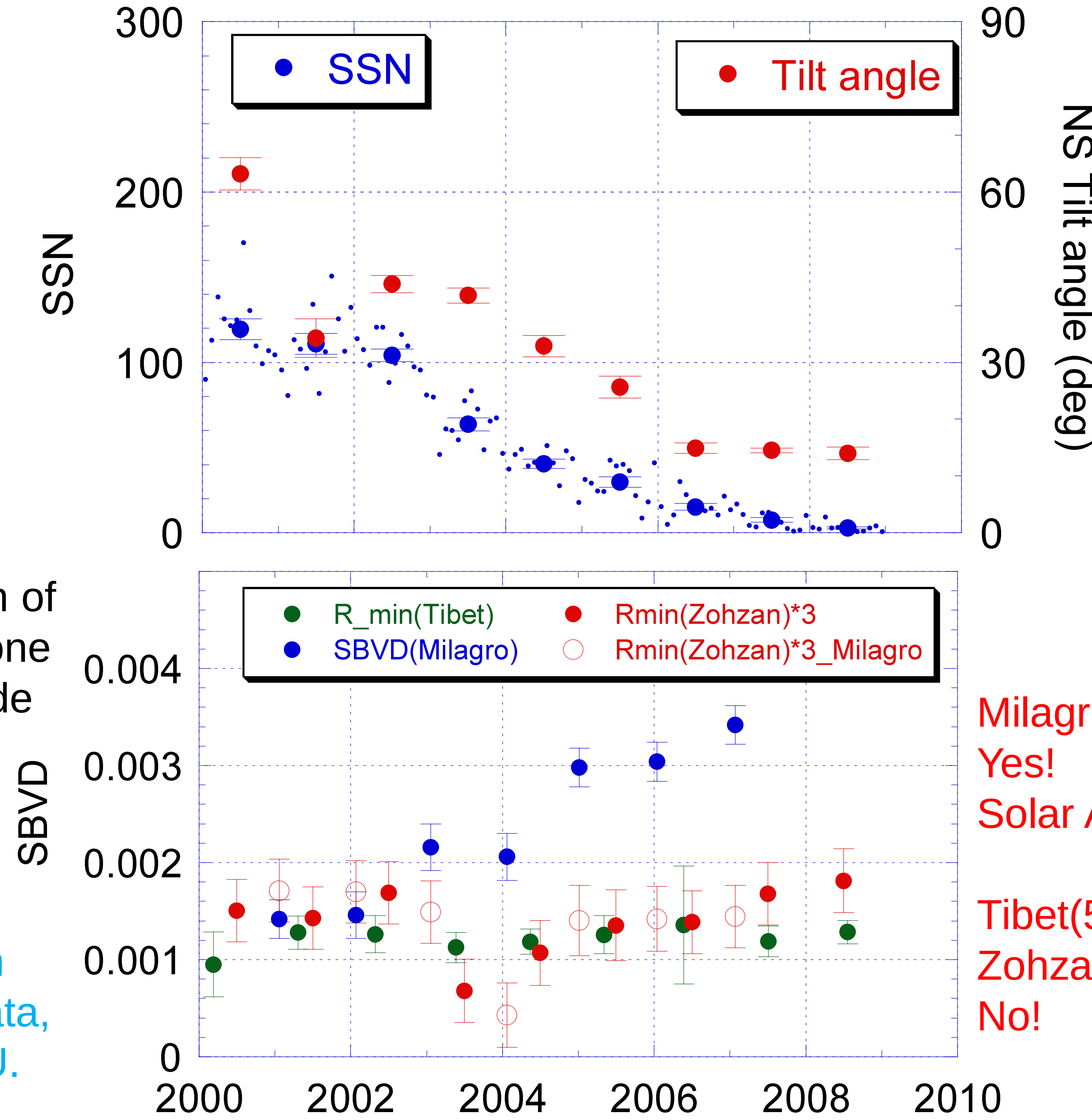

Milagro(6TeV)
Yes!
Solar Activities?

Tibet(5TeV)&
Zohzan(0.6TeV)
No!

Slide from K.Munakata, Shinshu U.

Yearly variation of Loss Cone amplitude

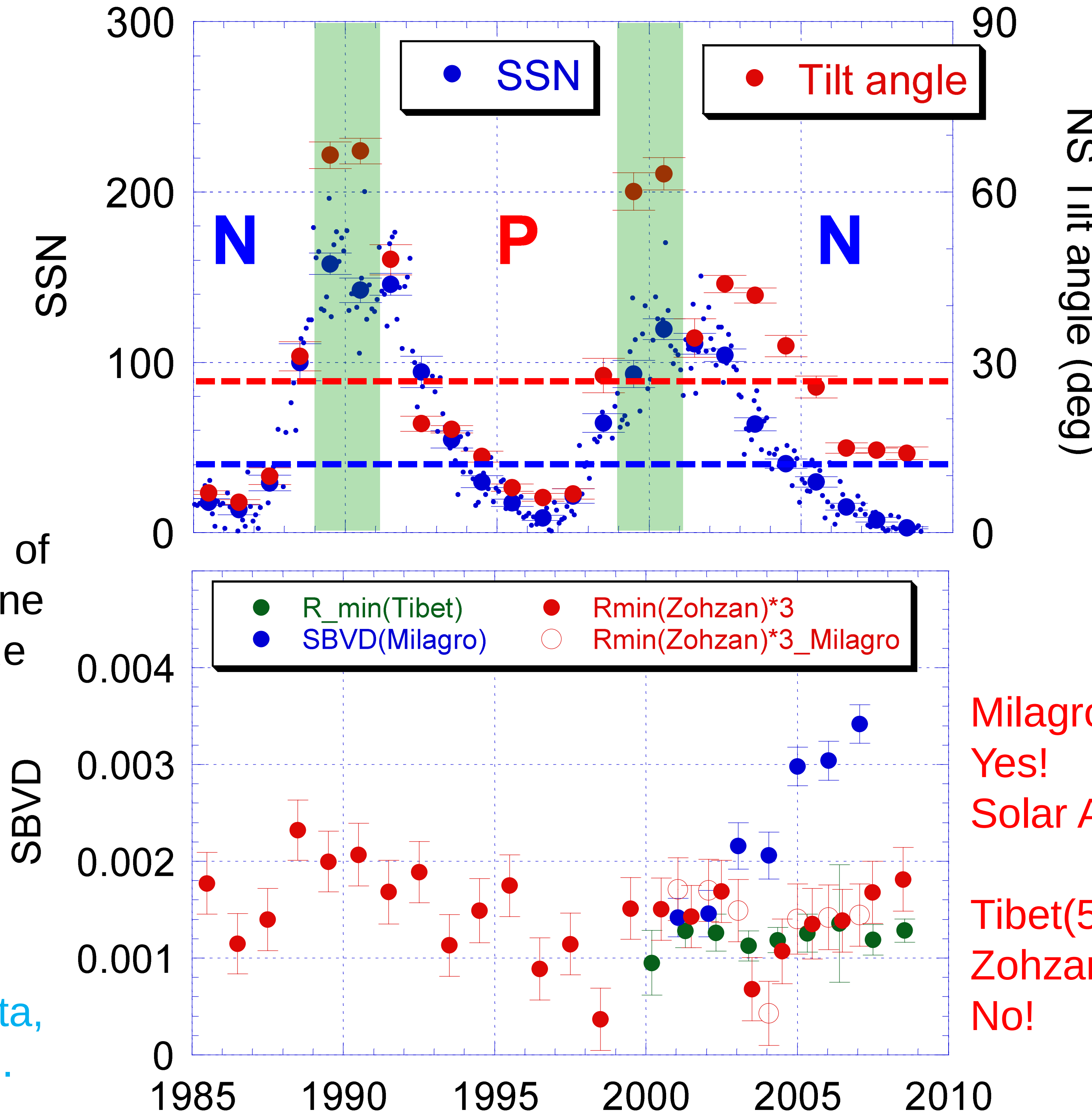

Milagro(6TeV)
Yes!
Solar Activities?

Tibet(5TeV)&
Zohzan(0.6TeV)
No!

Slide from
K.Munakata,
Shinshu U.

Observation of TeV Gamma Rays from the Fermi Bright Galactic Sources with the Tibet Air Shower Array (Amenomori et. al.)

Accepted by ApJ Letter

(arXiv:0912.0386)

Abstract

Using the Tibet-III air shower array, we search for TeV γ-rays from 27 potential Galactic sources in the early list of bright sources obtained by the *Fermi* Large Area Telescope at energies above 100 MeV. Among them, we observe 7 sources instead of the expected 0.61 sources at a significance of 2σ or more excess. The chance probability from Poisson statistics would be estimated to be 3.8×10^{-6}. If the excess distribution observed by the Tibet-III array has a density gradient toward the Galactic plane, the expected number of sources may be enhanced in chance association. Then, the chance probability rises slightly, to 1.2×10^{-5}, based on a simple Monte Carlo simulation. These low chance probabilities clearly show that the *Fermi* bright Galactic sources have statistically significant correlations with TeV γ-ray excesses. We also find that all 7 sources are associated with pulsars, and 6 of them are coincident with sources detected by the Milagro experiment at a significance of 3σ or more at the representative energy of 35 TeV. The significance maps observed by the Tibet-III air shower array around the *Fermi* sources, which are coincident with the Milagro $\geq3\sigma$ sources, are consistent with the Milagro observations. This is the first result of the northern sky survey of the *Fermi* bright Galactic sources in the TeV region.

Introduction

Large Area Telescope(LAT)
on the Fermi Gamma-Ray
Space Telescope

Lanched in June 2008

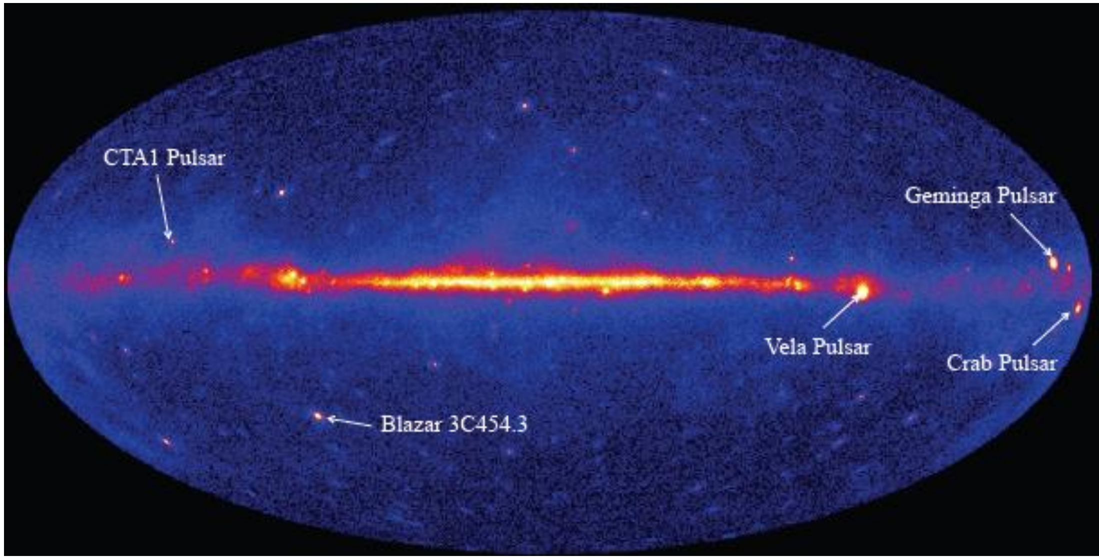

FERMI/LARGE AREA TELESCOPE BRIGHT GAMMA-RAY SOURCE LIST
Abdo, A. A. et al. 2009, ApJS, 183, 46 (July 2009, astrp-ph submitted in Feb. 2009)

Fermi LAT 3 month observation
>100MeV,
>10σ

205 most significant sources (120 extragalactic sourcs)
A typical 95% uncertainty radius of source position: 10′ ∼ 20′

Milagro Observation of TeV Emission from Galactic Sources
In the Fermi Bright Source List *(Abdo, A. A. et al 2009, ApJ, 700, L127)*

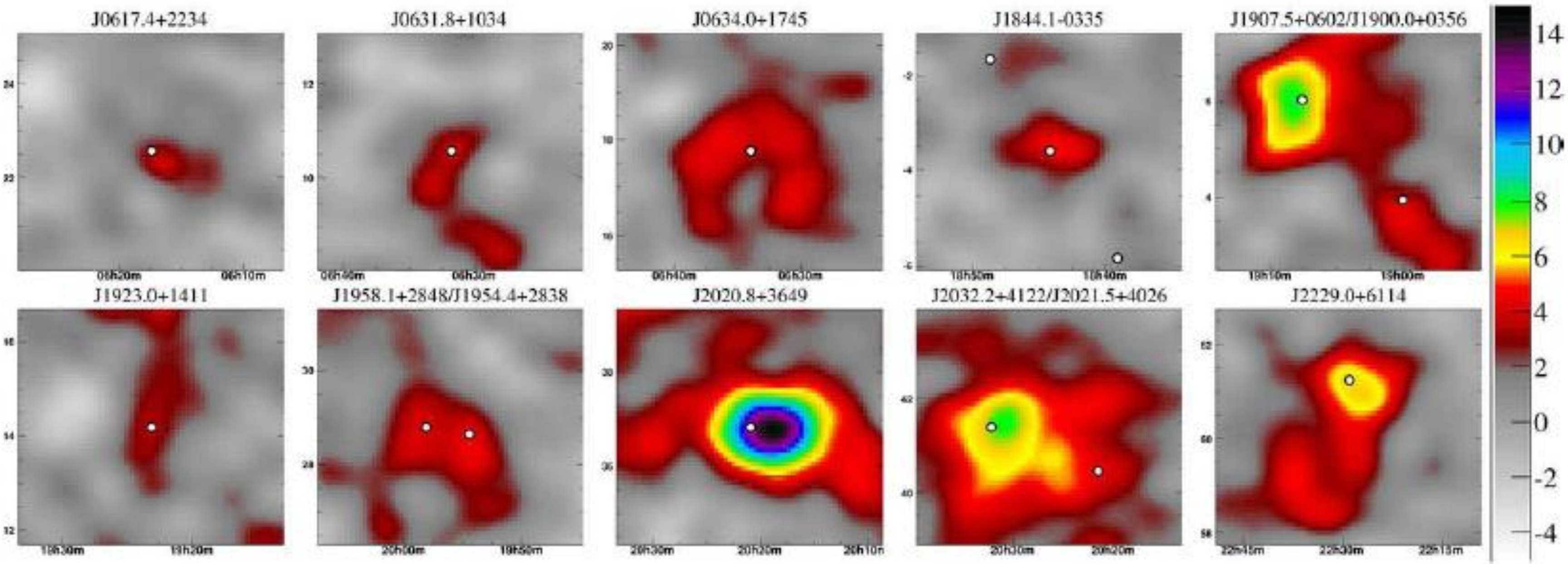

Fig. 1.— The 3σ sources from Table 1, omitting the Crab. Each frame shows a 5°x5° region with the LAT sources indicated by white dots. The data has been smoothed by a Gaussian of width varying between 0.4° and 1.0°, depending on the expected angular resolution of events. Horizontal axes show Right-Ascension and vertical axes show Declination. The colors indicate the statistical significance in standard deviations.

34 sources selected from 205 Fermi sources
(Not extragalactic & Dec.>-5.0º)

Eγ ~ 35 TeV

PSR	16
HXB	1
SRN	5
UNID	12

Milagro Results

Name (0FGL)	type	RA (deg)	DEC (deg)	l (deg)	b (deg)	Flux ($\times 10^{-17}$ TeV^{-1} sec^{-1} cm^{-2})	Signif. (σ's)	TeV assoc.
J0007.4+7303	PSR	1.85	73.06	119.69	10.47	< 90.4	2.6	
J0030.3+0450	PSR	7.60	4.85	113.11	-57.62	< 20.9	-1.7	
J0240.3+6113	HXB	40.09	61.23	135.66	1.07	< 26.2	0.7	LSI +61 303
J0357.5+3205	PSR	59.39	32.08	162.71	-16.06	< 16.5	-0.1	
J0534.6+2201	PSR	83.65	22.02	184.56	-5.76	162.6 ± 9.4	17.2	Crab
J0613.9-0202	PSR	93.48	-2.05	210.47	-9.27	< 60.0	-0.0	
J0617.4+2234	SNR[a]	94.36	22.57	189.08	3.07	28.8 ± 9.5	3.0	IC443
J0631.8+1034	PSR	97.95	10.57	201.30	0.51	47.2 ± 12.9	3.7	
J0633.5+0634	PSR	98.39	6.58	205.04	-0.96	< 50.2	1.4	
J0634.0+1745	PSR	98.50	17.76	195.16	4.29	37.7 ± 10.7	3.5	MGRO C3 Geminga
J0643.2+0858		100.82	8.98	204.01	2.29	< 30.5	0.3	
J1653.4-0200		253.35	-2.01	16.55	24.96	< 51.0	-0.5	
J1830.3+0617		277.58	6.29	36.16	7.54	< 32.8	0.2	
J1836.2+5924	PSR	279.06	59.41	88.86	25.00	< 14.6	-0.9	
J1844.1-0335		281.04	-3.59	28.91	-0.02	148.4 ± 34.2	4.3	
J1848.6-0138		282.16	-1.64	31.15	-0.12	< 91.7	1.7	
J1855.9+0126	SNR[a]	283.99	1.44	34.72	-0.35	< 89.5	2.2	
J1900.0+0356		285.01	3.95	37.42	-0.11	70.7 ± 19.5	3.6	
J1907.5+0602	PSR	286.89	6.03	40.14	-0.82	116.7 ± 15.8	7.4	MGRO J1908+06 HESS J1908+063

14 sources were detected with >3σ

J1911.0+0905	SNR[a]	287.76	9.09	43.25	-0.18	< 41.7	1.5	
J1923.0+1411	SNR[a]	290.77	14.19	49.13	-0.40	39.4 ± 11.5	3.4	HESS J1923+141
J1953.2+3249	PSR	298.32	32.82	68.75	2.73	< 17.0	0.0	
J1954.4+2838	SNR[a]	298.61	28.65	65.30	0.38	37.1 ± 8.6	4.3	
J1958.1+2848	PSR	299.53	28.80	65.85	-0.23	34.7 ± 8.6	4.0	
J2001.0+4352		300.27	43.87	79.05	7.12	< 12.1	-0.9	
J2020.8+3649	PSR	305.22	36.83	75.18	0.13	108.3 ± 8.7	12.4	MGRO J2019+37
J2021.5+4026	PSR	305.40	40.44	78.23	2.07	35.8 ± 8.5	4.2	
J2027.5+3334		306.88	33.57	73.30	-2.85	< 16.0	-0.2	
J2032.2+4122	PSR	308.06	41.38	80.16	0.98	63.3 ± 8.3	7.6	TEV 2032+41 MGRO J2031+41
J2055.5+2540		313.89	25.67	70.66	-12.47	< 17.6	-0.0	
J2110.8+4608		317.70	46.14	88.26	-1.35	< 24.1	1.1	
J2214.8+3002		333.70	30.05	86.91	-21.66	< 20.7	0.6	
J2229.0+6114	PSR	337.26	61.24	106.64	2.96	70.9 ± 10.8	6.6	MGRO C4
J2302.9+4443		345.75	44.72	103.44	-14.00	< 13.2	-0.6	

Tibet-III Data Analysis

All-sky Data by the Tibet-III Array (Phase 1-9 Ver.B4)

$\Sigma\rho_{FT} > 10^{1.25}$ && zenith <40°
Inout && 1.25p Any4 && Residual Error <1.0m
Search Window Size: $R_s(\Sigma\rho_{FT}) = 6.9 / \sqrt{\Sigma\rho_{FT}}$ (Variable)

1999 Nov – 2008 Dec
1915.5 live days

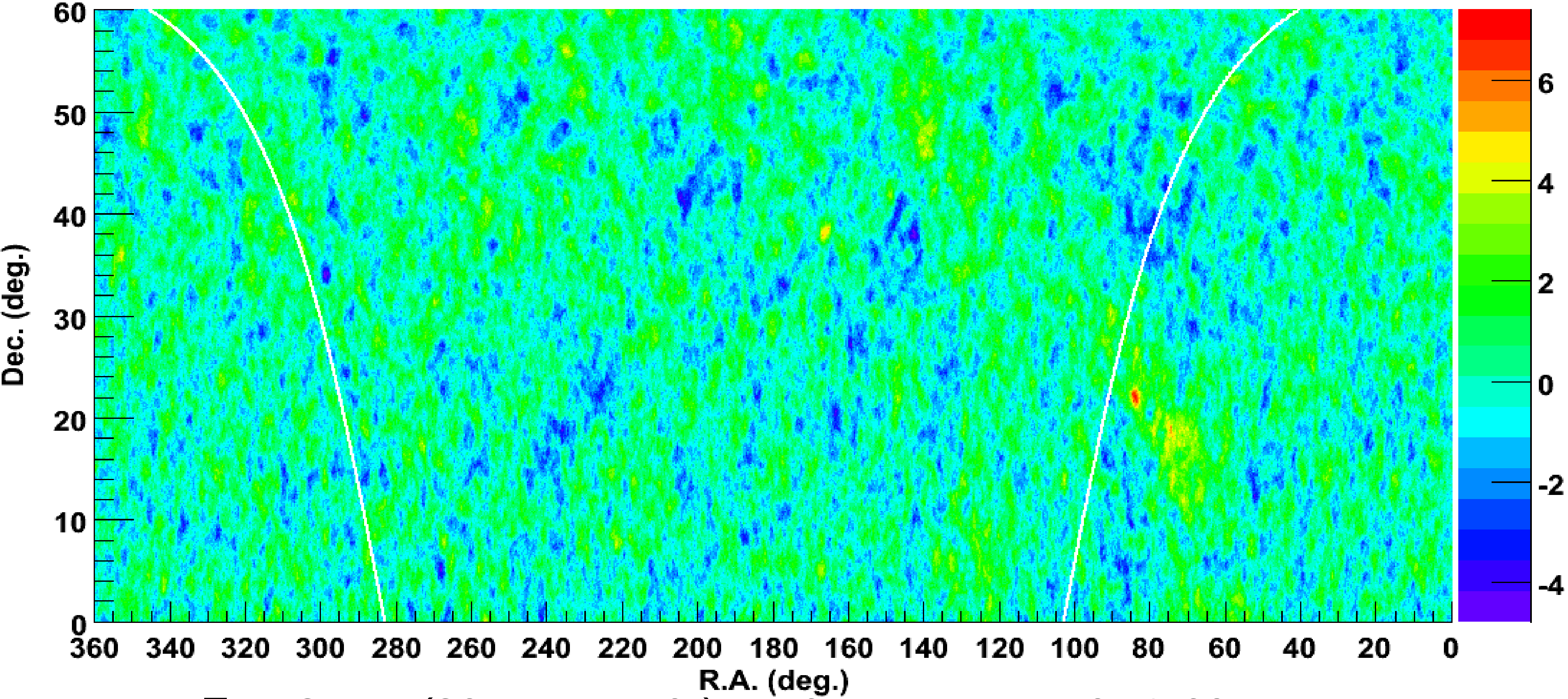

Eγ∼3 TeV (20°<Dec.<40°), ∼6 TeV at Dec.=0° & 60°

Target sources in the Fermi Bright Source List

The Fermi Bright Source List: 205 sources

Not identified as extragalactic: 85 sources

0^o < Declination < 60^o : 27 sources

Pulsar (PSR)	13
Supernova remnant (SNR)	5
Unidentified	9

Table 1
Summary of the Tibet-III Array Observations of the *Fermi* Sources

Fermi LAT Source (0FGL)	Class	R.A. (deg)	Decl. (deg)	Tibet-III Signi. (σ)	Milagro[a] Signi. (σ)	Source Associations
J0030.3+0450	PSR	7.600	4.848	1.7	−1.7	
J0357.5+3205	PSR[b]	59.388	32.084	−1.7	−0.1	
J0534.6+2201	PSR	83.653	22.022	6.9	17.2	Crab
J0617.4+2234	SNR	94.356	22.568	0.2	3.0	IC 443
J0631.8+1034	PSR	97.955	10.570	0.3	3.7	
J0633.5+0634	PSR[b]	98.387	6.578	2.4	1.4	
J0634.0+1745	PSR	98.503	17.760	2.2	3.5	Geminga
J0643.2+0858		100.823	8.983	−1.2	0.3	
J1830.3+0617		277.583	6.287	−0.2	0.2	
J1836.2+5924	PSR[b]	279.056	59.406	−0.3	−0.9	
J1855.9+0126	SNR	283.985	1.435	0.7	2.2	W44
J1900.0+0356		285.009	3.946	1.0	3.6	
J1907.5+0602	PSR[b]	286.894	6.034	2.4	7.4	MGRO J1908+06 HESS J1908+063
J1911.0+0905	SNR	287.761	9.087	1.7	1.5	G43.3 − 0.2
J1923.0+1411	SNR	290.768	14.191	−0.3	3.4	W51 HESS J1923+141

Geminga

Tibet-III 2σ
～0.3 Crabs

Table 1

Summary of the Tibet-III Array Observations of the *Fermi* Sources

Tibet-III 2σ～0.3 Crabs

Fermi LAT Source (0FGL)	Class	R.A. (deg)	Decl. (deg)	Tibet-III Signi. (σ)	Milagro[a] Signi. (σ)	Source Associations
J1953.2+3249	PSR	298.325	32.818	−0.0	0.0	
J1954.4+2838	SNR	298.614	28.649	0.6	4.3	G65.1+0.6
J1958.1+2848	PSR[b]	299.531	28.803	0.1	4.0	
J2001.0+4352		300.272	43.871	−0.5	−0.9	
J2020.8+3649	PSR	305.223	36.830	2.2	12.4	MGRO J2019+37
J2021.5+4026	PSR[b]	305.398	40.439	2.2	4.2	
J2027.5+3334		306.882	33.574	−0.3	−0.2	
J2032.2+4122	PSR[b]	308.058	41.376	2.4	7.6	TeV J2032+4130 MGRO J2031+41
J2055.5+2540		313.895	25.673	−0.0	−0.0	
J2110.8+4608		317.702	46.137	0.3	1.1	
J2214.8+3002		333.705	30.049	−1.0	0.6	
J2302.9+4443		345.746	44.723	−0.0	−0.6	
LAT PSR J2238+59[c]	PSR[b]	339.561	59.080	2.5	4.7	

Cygnus region

All 7 sources >2σ are associated with pulsars. →PWNs?
Six of them are coincident with Milagro sources.
Remaing one have still positive significance 1.4σ by Milagro.

New Fermi-LAT Pulsar, Not included in analysis

Statistics

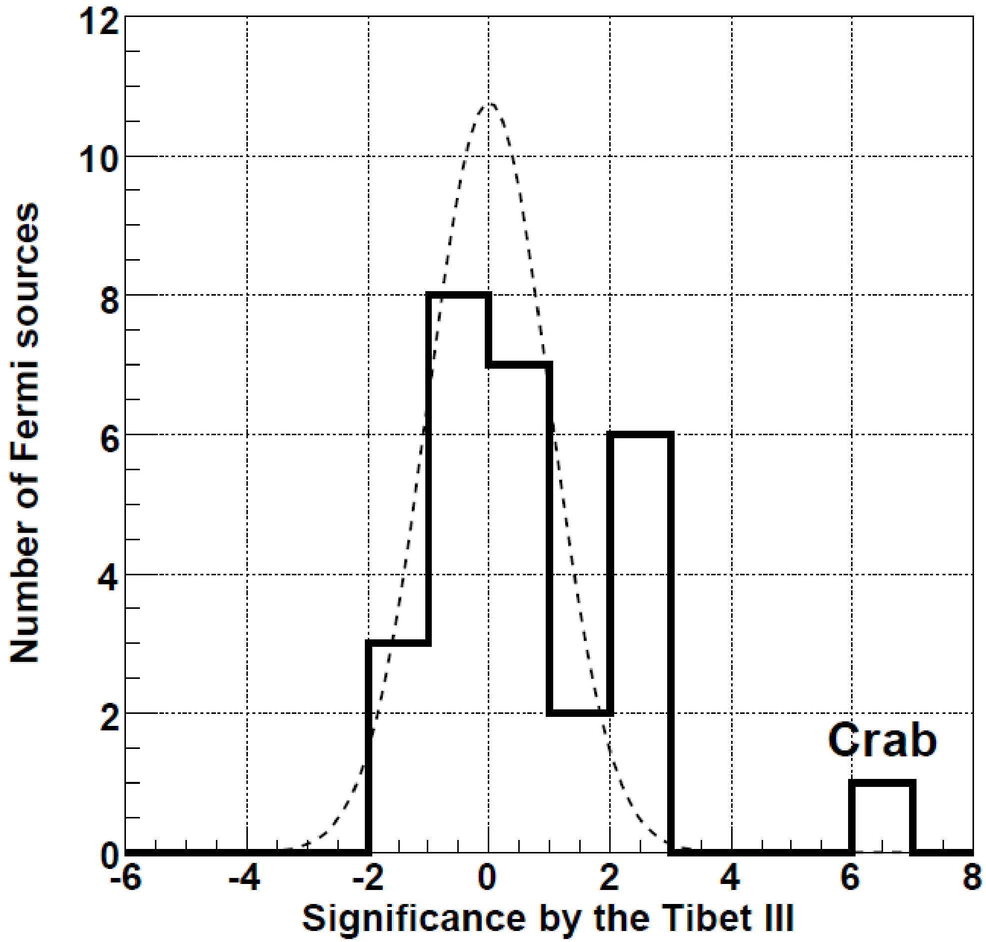

Total: 27 sources

>2σ: 7 sources

Fig. 1.— Histograms show significance distribution of the *Fermi* bright sources observed by the Tibet-III array. The dashed curve indicates the expected normal Gaussian distribution.

Chance Probability

Expected number of sources >2σ
27 × 0.02275 (2σ Upper prob.) = 0.61

Upper probabiriy for 7 events against λ=0.61
assuming Poisson statistics

$$p(A=7) = 1 - \sum_{k=0}^{A-1} \frac{e^{-\lambda} \lambda^{k}}{k!}$$

$$= 3.8 \times 10^{-6} \sim 4.5\sigma$$

Without Crab
λ = 26 × 0.02275 (2σ Upper prob.) = 0.59
P(A=6) = 3.6 × 10^{-5} ∼ 4σ

Flux consistency between the Tibet-III and the Milagro

	Tibet σ	Milagro σ	Expected σ from Milagro
J0534.6+2201	6.9	17.2	-
J0633.5+0634	2.4	1.4	0.56
J0634.0+1745	2.2	3.5	1.40
J1907.5+0602	2.4	7.4	2.97
J2020.8+3649	2.2	12.4	4.97
J2021.5+4026	2.2	4.2	1.68
J2032.2+4122	2.4	7.6	3.05

Underestimated?

J2020.8+3649 flux:
Tibet-III (30±14)% of the Crab flux above 3 TeV
Milagro (67±7)% of the Crab flux above 35 TeV

Δ = 2.3σ

difference between them is calculated to be 2.3σ. It can be interpreted by either statistical fluctuation, harder energy spectrum than the Crab, or an extended source instead of the assumed point-like source in this analysis.

Tibet-III

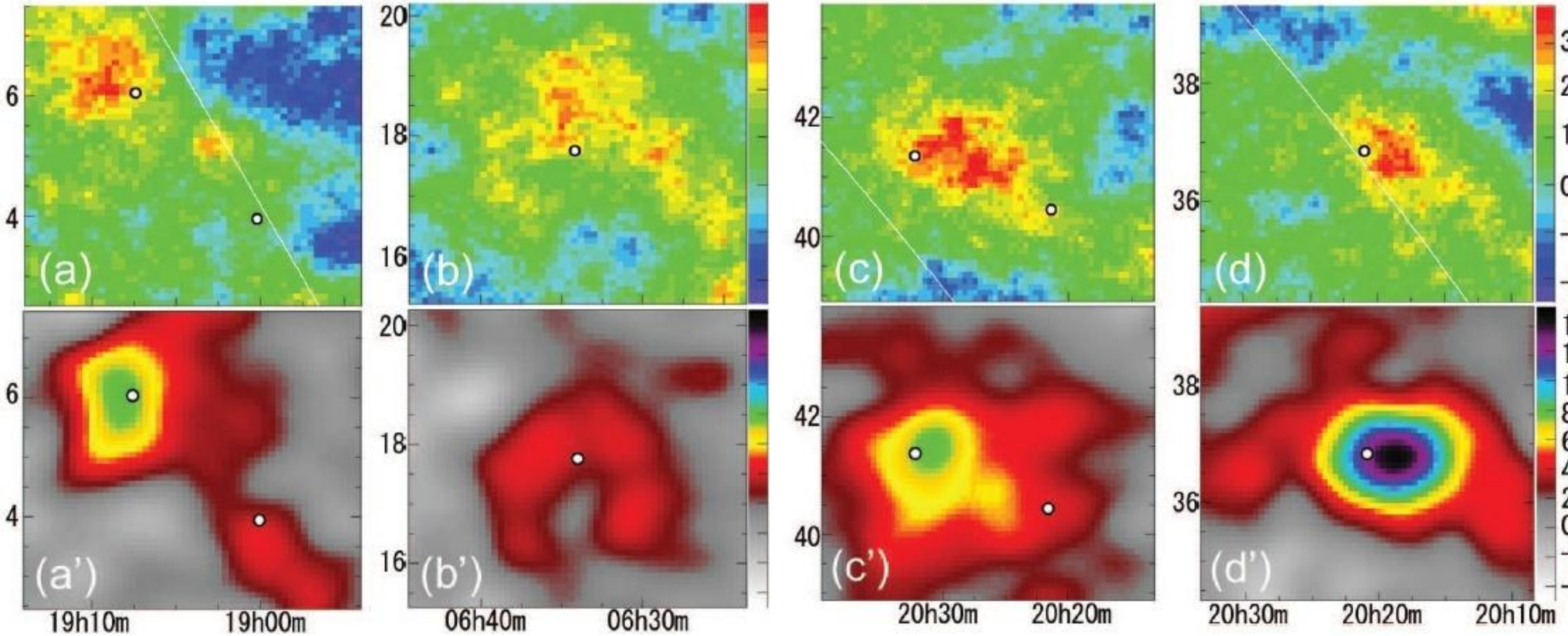

Milagro

Fig. 2.— Comparisons of significance maps around the *Fermi* sources between the Tibet-III array (a)–(d) and the Milagro experiment (a')–(d') taken from Abdo et al. (2009c). Selected are *Fermi* sources with $\geq 2\sigma$ significance by the Tibet-III array and $\geq 3\sigma$ by the Milagro experiment except for the Crab. White points in each image show the *Fermi* source positions: (a)(a') J1907.5+0602/J1900.0+0356; (b)(b') J0634.0+1745 (Geminga); (c)(c') J2021.5+4026/J2032.2+4122; (d)(d') J2020.8+3649. The horizontal axis, vertical axis, and color contours indicate the right ascension, declination, and significance, respectively.